The Reaction of Methyl Fluoroformyl Peroxycarbonate ($FC(O)OOC(O)OCH_3$) With Cl Atoms: Formation of Hydro-ChloroFluoro-Peroxides

Journal:	*The Journal of Physical Chemistry*
Manuscript ID	jp-2017-07449j.R2
Manuscript Type:	Article
Date Submitted by the Author:	15-Sep-2017
Complete List of Authors:	Berasategui, Matias; Universidad Nacional de Córdoba, Physical Chemistry Argüello, Gustavo; Universidad Nacional de Córdoba, Physical Chemistry Burgos Paci, Maxi; Universidad Nacional de Córdoba, Physical Chemistry

The Reaction of Methyl Fluoroformyl Peroxycarbonate ($FC(O)OOC(O)OCH_3$) with Cl Atoms: Formation of Hydro-ChloroFluoro-Peroxides.

*Matias Berasategui, Gustavo A. Argüello and Maxi A. Burgos Paci**

Instituto de Investigaciones en Físico Química de Córdoba (INFIQC) CONICET-UNC, Departamento de Físico Química, Facultad de Ciencias Químicas, Universidad Nacional de Córdoba, Ciudad Universitaria, X5000HUA Córdoba, Córdoba,

*Corresponding Author: mburgos@fcq.unc.edu.ar

ABSTRACT The products following Cl atom initiated reactions of $FC(O)OOC(O)OCH_3$ in 50-760 Torr of N_2 at 296 K were investigated using FTIR. Reaction of Cl atoms with methyl fluoroformyl peroxycarbonate proceeds mainly via attack at the methyl group, forming $FC(O)OOC(O)OCH_2^{\cdot}$ radicals. Further reaction of this kind of radicals with Cl_2 forms three new compounds: $FC(O)OOC(O)OCH_2Cl$; $FC(O)OOC(O)OCHCl_2$ and $FC(O)OOC(O)OCCl_3$, whose existence was characterized experimentally by FTIR spectroscopy assisted with ab-initio calculations at the B3LYP/6-31++G(d,p) level. Relative rate techniques were used to measure $k_{(Cl + FC(O)OOC(O)OCH3)} = (4.0 \pm 0.4) \times 10^{-14}$ cm^3 $molecule^{-1}$ s^{-1} and $k_{(Cl + FC(O)OOC(O)OCH2Cl)} = (3.2 \pm 0.3) \times 10^{-14}$ cm^3 $molecule^{-1}$ s^{-1}. When the reaction is run in presence of oxygen the paths giving chlorinated peroxide formation are suppressed and oxidation to (mainly) CO_2 and HCl takes place through highly oxidized intermediates with lifetimes long enough to be detected by FTIR spectroscopy.

1. Introduction

The use of hydrofluorocarbons (HFCs) in the last two decades has promoted exhaustive studies of the mechanisms, intermediates, and final products of the degradation reactions of this kind of compounds.[1] Also, in the past two decades, much work has been devoted to the study of the properties and reactions of many compounds and radicals containing only F, C, and O atoms, that can be formed in the laboratory as a result of the degradation of HFCs in the presence of oxygen and high concentrations of CO. The study of these reactions afforded many new compounds to be synthesized and used as precursors of atmospherically relevant radicals which were thus isolated.[2-4] Several such compounds have been known for many years (e.g., $CF_3OC(O)OOCF_3$[5] and $FC(O)OOC(O)F$[6]), and many others have been discovered and characterized recently (e.g., $CF_3OC(O)OOC(O)OCF_3$,[7] $CF_3OC(O)OOOC(O)OCF_3$,[8] $CF_3OC(O)OOC(O)F$,[9] and $FC(O)OOOC(O)F$[10]).

Methyl fluoroformyl peroxycarbonate ($FC(O)OOC(O)OCH_3$) is synthesized from the thermal reaction between $FC(O)OOC(O)F$ and CH_3OH, and it has been isolated and characterized recently.[11] Such molecule is of interest since it couples a fluorinated and a hydrogenated radical together, whose combined properties could therefore represent a transition from a purely fluorocarbooxygenated molecule to a hydrogenated one. Its thermal decomposition has been studied by Berasategui et al.[12] The rate constants of the homogeneous first-order thermal decomposition fits the Arrhenius equation $k_{exp} = (5.4 \pm 0.2) \times 10^{14}$ s^{-1} exp[−(27.1 ± 0.6 kcal mol^{-1}/RT)]. The proposed mechanism for the thermal decomposition goes through a loose transition state where the O—O bond cleavage takes place to produce CH_3OCO_2 and FCO_2 radicals.

On the other hand, extensive studies on the oxidation of volatile organic compounds (VOCs) initiated by Cl radicals are performed continuously and are highly significant in atmospheric chemistry.[13-18] Chlorine atom initiated oxidation of VOCs contribute to the generation of ozone and organic aerosols in the coastal areas and marine boundary layer, nevertheless many recent studies have emphasized the significant role of Cl atom as an oxidant in polluted urban atmospheres.[19-21] According to the first steps of the mechanisms the reaction of Cl atoms with VOCs is similar to that of OH radical, because they proceed through H abstraction from the alkyl groups or addition to double bonds in unsaturated hydrocarbons. However, the rate constants for Cl reactions are about one order of magnitude higher than those for OH.[22]

In this paper we present the results of the reaction of Cl atoms with $FC(O)OOC(O)OCH_3$. Rate constants for the replacement of H by Cl in the CH_3 fragment were measured, the new chlorinated molecules were detected by FTIR spectroscopy and their identification was assisted by *Ab-initio* calculations. The mechanism of the reactions sequence is discussed and supported with a kinetic model simulation.

2. Experimental Section

Caution! Although this study was conducted without mishap, it is important to take appropriate safety precautions when manipulating peroxyfluorinated compounds. Reactions involving these substances should be carried out only in millimolar quantities.

2.1. Instrumentation.

(a) Vibrational Spectroscopy. Gas-phase infrared spectra in the range of 4200–550 cm^{-1} were recorded with a resolution of 2 cm^{-1} from 32 co-added interferograms using a FTIR instrument (Bruker IFS66V).

(b) Nd: YAG Laser. A Q-switched pulsed Nd-YAG laser (Quantel, Brilliant B) was used as a photolizing source of Cl_2. It was operated at a repetition rate of 10 Hz with 5 nsec pulse width. The Nd: YAG laser is coupled with second (SHG) and third harmonic generation (THG) modules for producing 532 and 355 nm pulses. It was operated at a regime where only single photon absorption takes place. The photoreactions were initiated with the THG and the corresponding maximum output energy was about 200 mJ. The size of the photolysis beam was ~7×7 mm and the volume ratio (irradiated / cell) is 0.16. If we consider a cross section of $1.65x10^{-19}$ cm^2/molecule for the absorption of Cl_2 at 355nm and ϕ=1 for the reaction Cl_2 + hν(355nm)→ 2 Cl, then the total density of Cl atoms produced in the irradiated volume after each pulse was ~$4.8x10^{15}$ molecules cm^{-3} which is three orders smaller than the total density of Cl_2 at 100 mbar (~$2.4x10^{18}$ molec cm^{-3}).

(c) Computational Details. First principles calculations were carried out using the MP2 and B3LYP methods in combination with different basis sets. They are specified in the First Principle Calculation section for each system. The highly accurate energy method Gaussian-2 (G2)[23] was used for the calculation of thermodynamic properties. All calculations were run with the Gaussian 09[24] program package.

2.2. General Procedures.

Volatile materials were manipulated in a glass vacuum line equipped with two capacitance pressure gauges (0-760 Torr, MKS Baratron; 0-70 mbar, Bell and Howell), three U traps, and valves with poly(tetrafluoroethylene) stems (Young, London). The vacuum line was connected to a stainless steel reactor which had in parallel a double-jacketted stainless steel IR gas cell (optical path length 200 mm, KBr windows) placed in the sample compartment of a Fourier transform infrared (FTIR) instrument. The cell and the reactor were interconnected by PTFE pipes through Swagelok's valves and connectors. This arrangement made it possible to follow either the course of the synthesis or the purification of substances.

As the $FC(O)OOC(O)OCH_3$ decomposition is catalyzed in the presence of Si-containing surfaces, the photochemical reactions were performed in stainless steel reactors, thus avoiding any contact with glass surfaces. The reaction was investigated by irradiating $FC(O)OOC(O)OCH_3/Cl_2$ mixtures at 800 Torr of total pressure of N_2 at 296 ± 2 K. The Nd-YAG laser was used to start the bond cleavage reaction of Cl—Cl. The laser beam went in and out the cell through KBr windows. After 150 pulses (which correspond to 750 ns of net irradiation during a lapse of 15 seconds), the cell was placed in the optical path of the FTIR

equipment, and its content was analyzed. This procedure was repeated until completion of the experiment.

Most of the products obtained (CO_2, CO, HF, HCl, etc.) were identified and quantified from reference spectra of pure samples.

2.3. Chemicals.

The synthesis of $FC(O)OOC(O)OCH_3$ was carried out following the recipe in[11]. Briefly, the reactor was loaded with CH_3OH and an excess of FC(O)OOC(O)F. The reaction stopped when CH_3OH was consumed at about 30 min, then $FC(O)OOC(O)OCH_3$ was distilled in situ by immersion of the whole reactor in ethanol baths at −100 and −60 °C to carefully remove excess of FC(O)OOC(O)F and byproducts. With this method the purity of the sample was better than 98%. Cl_2 was obtained from the liquid phase reaction between $KMnO_4$ and concentrated HCl, and purified in the glass vacuum line. Bath gases were obtained from commercial sources at the following purities: N_2 (>99.9%, Linde) and O_2 (>99.9%, Linde).

2.4 Determination of rate constants.

The rate constant of the reaction of Cl atoms with $FC(O)OOC(O)OCH_3$ was measured relative to different reference reactions with known rate constants. The relative rate method is a well-established technique for measuring the reactivity of Cl atoms with organic compounds[25]. Kinetic data are derived by monitoring the change of IR signal of the peroxyde relative to the change of a reference compound which could be CH_4, CH_2Cl_2 or $CHCl_3$. The decays of the reactant and reference are then plotted using the expression:

$$\ln([\text{Perox}]_{t0}/[\text{Perox}]_t) = k_{\text{Perox}}/k_{\text{ref}} \ln([\text{ref}]_{t0}/[\text{ref}]_t)$$

where $[\text{Perox}]_{t0}$, $[\text{Perox}]_t$, $[\text{ref}]_{t0}$ and $[\text{ref}]_t$ are the concentrations of peroxyde and reference at times 0 and t, k_{Perox} and k_{ref} are the rate constants for reactions of Cl atoms with the peroxyde and reference, respectively. Plots of $\ln([\text{Perox}]_{t0}/[\text{Perox}]_t)$ vs. $\ln([\text{ref}]_{t0}/[\text{ref}]_t)$ should be linear, pass through the origin and have a slope of $k_{\text{Perox}}/k_{\text{ref}}$. The loss of the reactant and reference compounds was monitored by FTIR spectroscopy within the 20 cm path length cell. The concentrations of reactant and reference compounds were determined with a precision of ± 1% of their initial concentrations. Initial reagent concentrations were 5–10 mTorr of peroxyde, 5–40 mTorr of reference, and 50–100 mTorr of Cl_2 and N_2 diluent at total pressure of 700 Torr. Every experiment consisted of filling the cell with a mixture of peroxyde/reference/Cl_2/N_2 and subjecting the mixture to the already mentioned 150 pulses of laser radiation. After each set of pulses, the chemical composition in the chamber was analyzed using FTIR spectroscopy.

3. Results and Discussion

3.1. Rate constant of the reaction (Cl + $FC(O)OOC(O)OCH_3$).

Cl atoms generated by photolysis

$$Cl_2 + h\nu \rightarrow 2\ Cl \qquad (1)$$

were used to study the kinetics between Cl and methyl fluoroformyl peroxycarbonate reaction (2). Three other reactions (3), (4) and (5), whose rate constants are well characterized have been used as reference reactions in order to minimize the error associated with k_2.

$Cl + FC(O)OOC(O)OCH_3 \rightarrow$ products (2)

$Cl + CH_4 \rightarrow$ products (3)

$Cl + CH_2Cl_2 \rightarrow$ products (4)

$Cl + CHCl_3 \rightarrow$ products (5)

The disappearance of the reagent was followed using the absorption band at 2973 and corroborated with the band at 1264 cm^{-1} corresponding to O-C-O vibration of the $CH_3OC(O)O$- group. This band is not overlapped with any absorption band of the products.

Figure 1 shows plots of the loss of $FC(O)OOC(O)OCH_3$ versus CH_4, CH_2Cl_2 and $CHCl_3$ following exposure to Cl atoms in 700 Torr of N_2 at 296 K. Linear least-squares analysis of the data gives rate constant ratios $k_2/k_3 = 0.3695 \pm 0.0022$; $k_2/k_4 = 0.1098 \pm 0.0012$ and $k_2/k_5 = 0.5359 \pm 0.0100$ (quoted errors are two standard deviations). The relative rate data can be placed upon an absolute basis using $k_3 = 1.08 \times 10^{-13}$, $k_4 = 3.57 \times 10^{-13}$ and $k_5 = 7.64 \times 10^{-14}$ [26] to give $k_2 = (3.99 \pm 0.02) \times 10^{-14}$, $(3.92 \pm 0.04) \times 10^{-14}$ and $(4.09 \pm 0.08) \times 10^{-14}$ cm^3 $molecule^{-1}$ s^{-1} (where the uncertainties come from the errors of the quotients). The values of k_2 obtained using the three different reference compounds were indistinguishable within the experimental uncertainties, suggesting the absence of substantial systematic errors associated with the use of individual reference reactions. We have chosen to quote a final value of k_2 which is the average of the individual measurements, estimating that potential systematic errors associated with uncertainties in the reference rate constants contribute an additional 10% to the uncertainty range. Hence, the final k_2 value would be $(4.0 \pm 0.4) \times 10^{-14}$ cm^3 $molecule^{-1}$ s^{-1}.

To get a better understanding of the mechanism of oxidation of $FC(O)OOC(O)OCH_3$, the reaction between Cl atoms and fluoro methyl formate was studied under similar conditions. The

synthesis of $FC(O)OCH_3$ was carried out following Burgos et al. recipe.[27] Relative rate experiments were performed to study the kinetic of reaction (6) relative to reactions (3) and (4).

$$Cl + FC(O)OCH_3 \rightarrow \text{products} \qquad (6)$$

Using the same arguments as for the peroxide for the bands at 1845 and 2974 cm^{-1} of $FC(O)OCH_3$, the rate constant found was $k_6 = (8.1 \pm 0.8) \times 10^{-14}$ cm^3 $molecules^{-1}$ s^{-1}. This value is within the order of magnitude to the one found for $FC(O)OOC(O)OCH_3$. The slight increase in the value of the rate constant may be an indication of its dependence on the group bounded to the common $CH_3OC(O)$- moiety.

3.2. Determination of intermediates and products of the reaction Cl + $FC(O)OOC(O)OCH_3$.

After the initiation of the photolysis HCl was detected at 2820 cm^{-1} and showed an increasing concentration with time. This is in fact, the expected result since it is well established that Cl atoms produce hydrogen abstraction from alkyl groups in saturated compounds.[18,22] Taking this into account, reaction (7) is proposed as the first step in the mechanism.

$$FC(O)OOC(O)OCH_3 + Cl \rightarrow FC(O)OOC(O)OCH_2 + HCl \qquad (7)$$

The alkyl radical $FC(O)OOC(O)OCH_2$ may decompose to form sub-products (as stated in reaction 8), or react with Cl_2 to generate a new chlorinated compound as indicated in reaction (9).

$$FC(O)OOC(O)OCH_2 \rightarrow 2\ CO_2 + CH_2O + F \quad (8)$$

$$FC(O)OOC(O)OCH_2 + Cl_2 \rightarrow FC(O)OOC(O)OCH_2Cl + Cl \quad (9)$$

Because neither CH_2O nor any other product ascribable to the oxidation of this radical was observed, the occurrence of reaction (8) was discarded. Other possibilities to consider in the system are radical-radical and radical-Cl reactions. To evaluate these possible reactions we run a simulation with initial concentrations of Cl_2, Cl and $FC(O)OOC(O)OCH_3$ taken from an experimental run. Because of the lack of rate constants to evaluate the mechanism, those of CH_3-CH_3 and CH_3-Cl were used, which could be taken as upper limits of the present reactions. Figure S1 shows the evolution of the system and it can be observed that 98% of the radicals undergo channel 9 in the time scale of the experiment.

The concentration of the initial peroxide was followed by its FTIR band at 2973 cm^{-1} because absorption at this region does not overlap with bands from products.

Figure 2 shows the IR absorption bands in the 1980 – 1150 cm^{-1} range at different extents of reaction. Spectrum "a" corresponds to the initial peroxide before the photoreaction is initiated; spectrum "b" was obtained after half of the reactant has disappeared (after the band at 2973 cm^{-1} was reduced to the half) and spectrum "c" was measured after $FC(O)OOC(O)OCH_3$ has completely disappeared. The sequence of spectra shows changes in the shape, intensities and frequencies of the bands. The two bands at 1834 and 1908 cm^{-1} are shifted to higher wavenumbers. In the range 1310 – 1360 cm^{-1} two new bands appear in trace "b" and change their relative intensities in trace "c". A new band appears at 1238 cm^{-1} and the high intensity band at 1190 cm^{-1} is red shifted to 1176 cm^{-1}. All these changes are a clear evidence of intermediates or

final species with enough lifetimes to be detected by FTIR that are produced in the course of the photolysis.

In order to explain the formation of intermediate species, the Cl atoms produced by reactions (1) and (9) could react in a chain reaction with the chlorinated peroxide formed in reaction (9) to replace the second and third hydrogen of the original $–CH_3$ fragment, according to reactions (10)-(13).

$$FC(O)OOC(O)OCH_2Cl + Cl \rightarrow FC(O)OOC(O)OCHCl + HCl \quad (10)$$

$$FC(O)OOC(O)OCHCl + Cl_2 \rightarrow FC(O)OOC(O)OCHCl_2 + Cl \quad (11)$$

$$FC(O)OOC(O)OCHCl_2 + Cl \rightarrow FC(O)OOC(O)OCCl_2 + HCl \quad (12)$$

$$FC(O)OOC(O)OCCl_2 + Cl_2 \rightarrow FC(O)OOC(O)OCCl_3 + Cl \quad (13)$$

As long as we are concerned, these three (mono, bi and tri)-Chloromethyl Fluoroformyl Peroxycarbonate molecules have not been reported yet.

The molecular structures and the infrared spectra of these peroxides were simulated using the B3LYP/6-311++G(d,p) level of theory. The molecular parameters for the most stable conformers are presented in Table S1. The most relevant structural parameters are the dihedral (O)C—O—O—C(O) and the peroxidic bond length O—O. These parameters have been measured by gas electron diffraction (GED) techniques for other peroxy-dicarbonyl compounds like $FC(O)OOC(O)F$[28], $CF_3C(O)OOC(O)CF_3$[29] and $CF_3OC(O)OOC(O)OCF_3$.[30] For the three peroxides only a single syn-syn conformation with both C=O bonds in syn orientations were observed by GED.[31] In the chlorinated peroxides here proposed, these orientations were also predicted for the most stable conformers. The dihedral angle C—O—O—C experimentally

found for peroxides with two sp^2 substituents are smaller than 90º, ie. 84(2)º in FC(O)OOC(O)F[28] and 87(2)º in $CF_3OC(O)OOC(O)OCF_3$[30]. For the chlorinated peroxides the values obtained from the calculations are 88.8º in $FC(O)OOC(O)OCH_2Cl$, 89.6º in $FC(O)OOC(O)OCHCl_2$ and 91.2º in $FC(O)OOC(O)OCCl_3$, that is, an increase of the dihedral with chlorine substitution. The O—O bond length for the new peroxides are 1.43 Å, slightly longer than the experimental value for the fluorinated peroxides which are between 1.403 – 1.426 Å. According to the theoretical method used for calculation of geometrical parameters, Oberhammer[31] has pointed that MP2 gives better results than B3LYP for FC(O)OOC(O)F but B3LYP gives better agreement with experiment than MP2 for $CF_3OC(O)OOC(O)OCF_3$. A systematic investigation with different theoretical methods and basis sets and GED studies of the present new peroxides are highly desirable.

Table S2 presents the calculated harmonic vibrational frequencies of the intermediates and final product, as well as our experimental results. The changes observed in the sequence of spectra shown in Fig 2 are in agreement with the mechanism proposed on account of the quantum calculations for the different peroxides. The C=O stretching experimental bands of $FC(O)OOC(O)OCH_3$ at 1834 and 1908 cm^{-1} appear at 1868 and 1947 cm^{-1} in the calculation. The corresponding bands calculated for $FC(O)OOC(O)OCH_2Cl$ are 1879 and 1950 cm^{-1}; for $FC(O)OOC(O)OCHCl_2$ are 1877 and 1953 and for $FC(O)OOC(O)OCCl_3$ are 1901 and 1955 cm^{-1}. Despite the error associated with the calculated frequencies, when the chlorination reaction evolves in time, it is expected that the bands at 1834 and 1908 shift to higher wavenumbers, as observed. The two low intensity bands observed at 1350 and 1325 cm^{-1} shown in figure 2 could be assigned to the H—C—Cl vibration of the intermediates mono and dichloro- respectively, since the calculated frequencies are 1387 and 1355 cm^{-1} for $FC(O)OOC(O)OCH_2Cl$ and

$FC(O)OOC(O)OCHCl_2$. Besides in the experimental sequence of spectra, the band at 1325 cm^{-1} grows up at the expense of the band at 1350 cm^{-1}, as expected considering the formation of the dichloride from the monochloride peroxide. The band observed in the experimental spectra at 1238 cm^{-1} can be attributable to the O—C—O vibration of the intermediates, since that mode is calculated at 1244 cm^{-1}. The frequencies calculated for the most intense band of each one of the peroxides are 1187 cm^{-1} for $FC(O)OOC(O)OCH_3$, 1180 cm^{-1} for both $FC(O)OOC(O)OCH_2Cl$ and $FC(O)OOC(O)OCHCl_2$ and 1162 cm^{-1} for $FC(O)OOC(O)OCl_3$. Then the sequential chlorination moves this band to the red, as is also experimentally observed.

3.3. Rate constants for the reactions between Cl and molecular intermediates $FC(O)OOC(O)OCH_2Cl$, $FC(O)OOC(O)OCHCl_2$.

The reaction of H atom abstraction by a Cl atom to form HCl and a radical is always followed by a faster reaction where the radical reacts with Cl_2 (due to its high concentration in the system) and forms either a partially chlorinated intermediate or the fully chlorinated $FC(O)OOC(O)OCl_3$ peroxide. In any case the rate determining step to the formation of these "stable" peroxides is always the reaction that forms HCl, that is, reactions 7, 10 and 12. With this in mind, the measurement of the concentration of each intermediate ($FC(O)OOC(O)OCH_2Cl$, $FC(O)OOC(O)OCHCl_2$) as function of reaction progress should give information about the kinetics. Nevertheless, the partially chlorinated peroxides are substances with peculiar time variations. Two methods were used to find the rate constant k_{10}. In the first one we used the approach described by Meagher et al.[32] to obtain the rate constant for a process where the same compound is used as a precursor and reference. In the present case this molecule is

$FC(O)OOC(O)OCH_3$. The functional form between the rate constants k_{10}/k_7 and the concentration of precursor and $FC(O)OOC(O)OCH_2Cl$ is given by the equation:

$$\frac{[FC(O)OOC(O)OCH_2Cl]_t}{[FC(O)OOC(O)OCH_3]_0} = \frac{\alpha}{1-{}^{k_{10}}/_{k_7}}(1-x)\left[(1-x)^{\left\{{}^{k_{10}}/_{k_7}-1\right\}}-1\right] \quad \text{(I)}$$

where x is defined as:

$$x = 1 - \frac{[FC(O)OOC(O)OCH_3]_t}{[FC(O)OOC(O)OCH_3]_0} \quad \text{(II)}$$

The value of α is the yield of $FC(O)OOC(O)OCH_2Cl$ from $FC(O)OOC(O)OCH_3$. In this system α was supposed to be approximately 1 because the only reaction of the radical $FC(O)OOC(O)OCH_2$ under the present conditions is the formation of $FC(O)OOC(O)OCH_2Cl$ (reaction 9) as was already mentioned. Figure 3 shows the plot of $[FC(O)OOC(O)OCH_2Cl]_t$ / $[FC(O)OOC(O)OCH_3]_0$ vs. $\Delta[FC(O)OOC(O)OCH_3]/[FC(O)OOC(O)OCH_3]_0$ with different pressures of Cl_2. The α parameter and the rate constant ratio k_{10}/k_7 were obtained using nonlinear fit of equation (I) to the experimental data shown in the figure. The experimental value found for α is (1.00 ± 0.02) which is in excellent agreement with the absence of CH_2O as a product in reaction (8). The value from the fitting for k_{10}/k_7 was (0.74 ± 0.02) and the rate constant k_{10} obtained from this method was (3.0 ± 0.1) × 10^{-14} cm^3 $molecules^{-1}$ s^{-1} (where the error limit corresponds to the standard deviation of the fitting).

The second procedure followed to calculate k_{10} was the following: it was assumed that the reagent reacted with Cl to form the monochlorinated peroxide which is deprived from decomposing. Thus, a curve was constructed that showed the amount of $FC(O)OOC(O)OCH_2Cl$ as a function of time that was an ever growing (eventually reaching a plateau) curve. The difference (at each measured time) of this curve with the actual concentration (given by the absorption band at 1350 cm^{-1}) indicated the amount of $FC(O)OOC(O)OCH_2Cl$ that had reacted

to form the dichlorinated peroxide. From these values, figure S2 was constructed taking the reagent, CH_4 or CH_2Cl as reference compounds, the slope returned the rate constant relative to the each reference. Interesting to note is the consistence of the values measured at different initial pressures and even with different IR bands. Using the least squares method from the linear regression for each reference we obtained the quotient for the rate constants $k_{10}/k_7 = 0.86 \pm 0.09$, $k_{10}/k_3 = 0.321 \pm 0.004$ and $k_{10}/k_4 = 0.092 \pm 0.002$. Considering the experimental values of k_7, k_3 and k_4, and using a similar approach, already mentioned for k_7, we found the value for the rate constant of the reaction $FC(O)OOC(O)OCH_2Cl + Cl$, $k_{10} = (3.4 \pm 0.3) \times 10^{-14}$ cm^3 molec^{-1} s^{-1}.

The two values of k_{10} obtained from the different methods are in agreement within experimental errors. Taking an average of both values, the rate constant k_{10} has a value of $(3.2 \pm 0.3) \times 10^{-14}$ cm^3 molec^{-1} s^{-1} with a 10% error. This rate constant is slightly lower than the one found for reaction (7), so the concentration of the intermediate will never reach higher than the concentration of $FC(O)OOC(O)OCH_3$.

Based on the rate constants found for reactions (7) and (10), we performed a kinetic simulation considering all the reactions involved using the Kintecus program package.[33] For reactions (9), (11) and (13) we used bibliographic rate constant values for similar radicals (NIST,[34] $k_{CH3 + Cl2} = 1.55 \times 10^{-12}$ cm^3 molecule^{-1} s^{-1},[35] $k_{CH2Cl + Cl2} = 2.54 \times 10^{-13}$ cm^3 molecule^{-1} s^{-1},[36] and $k_{CHCl2 + Cl2} = 2.25 \times 10^{-14}$ cm^3 molecule^{-1} s^{-1}),[37] and for the thermal decomposition we used the rate constant obtained by Berasategui et al.[12] Besides, the experimental concentration of reagent, intermediates and products were introduced in the model; HCl, CO_2 and $FC(O)OOC(O)OCH_3$ were quantified using the integration of the bands at ~2820, ~2358 and 2973 cm^{-1} respectively. The concentration of the intermediate $FC(O)OOC(O)OCHCl_2$ was obtained using the experimental band at 1325 cm^{-1}. Using these data as input parameters, the Kintecus program solved the kinetic equations

with k_{12} as the only variable. Figure 4 presents the variation in concentrations of the reactant, intermediates and products involved in the mechanism as a function of the progress of reaction. The experimental points are represented by squares, diamonds, etc., while the curves result from the simulation with the mechanism proposed. The concentrations of the intermediates $FC(O)OOC(O)OCH_2Cl$ and $FC(O)OOC(O)OCHCl_2$ were estimated from the comparison of the absolute maxima of the simulation curves. Table 1 presents the reactions and the rate constants used for each step. It is important to highlight the remarkable matching of the simulation with the experimental evolution. From this, we obtained the rate constant for reaction (12) to be $k_{12} = (1.7 \pm 0.6) \times 10^{-14}$ cm^3 molecule^{-1} s^{-1}.

It can be seen from figure 4 that HCl concentration grows monotonically and its concentration at t_∞ is three times the concentration of $FC(O)OOC(O)OCH_3$ and the concentration of the intermediates evolve as expected for consecutive reactions. On the other hand, the appearance of CO_2 and Cl_2CO after 70% consumption of $FC(O)OOC(O)OCH_3$ is an indicative of reaction (14).

$$FC(O)OOC(O)OCCl_2 \rightarrow CCl_2O + 2\ CO_2 + F \qquad (14)$$

The exothermicity of (14), calculated with B3LYP/6-31++G(d,p), is 20 kJ mol^{-1} higher than that for reaction (8), which may explain why CCl_2O and CO_2 appear at long times in the system while no CH_2O was observed. Reaction (14) was also included in the mechanism and the simulated unimolecular rate constant was 1.5×10^5 s^{-1}.

For the group of molecules studied in this work, it is evident that the rate constant for the abstraction of one hydrogen from a H_3C— fragment is higher than for a H_2CCl—, which is higher than for $HCCl_2$—, the same is observed for $ClC(O)OCH_3$ (1.1×10^{-13} cm^3 molecule^{-1} s^{-1}) and $ClC(O)OCH_2Cl$ (3.0×10^{-14} cm^3 molecule^{-1} s^{-1}).[38] Steric and electronic effects should be

taken into account to analyze this tendency, the former being evident because the exposure of a hydrogen atom is in some way "shielded" by chlorine after the first replacement has taken place, and the last effect shows that the H—C covalent bond is weakened by the presence of atoms with high electronegativity bonded to the same carbon.

3.4. Additional mechanistic studies from the products of Cl initiated oxidation of $FC(O)OOC(O)OCH_3$ in presence of O_2.

In order to investigate the products of the Cl atom initiated oxidation of methyl fluoroformyl peroxycarbonate, we performed experiments in which $FC(O)OOC(O)OCH_3/Cl_2/O_2/N_2$ mixtures were exposed to UV laser irradiation. IR spectra were acquired after each period of irradiation. Experiments were performed at a total pressure of 760 Torr, with O_2 partial pressure higher than 50 going up to 250 Torr. The main products identified were: HCl, HF, CO and CO_2. Figure 5 shows the initial (before exposure to UV light) and the final spectra.

Under these experimental conditions the reaction showed no indication of the formation of any chlorinated peroxide, so the occurrence of reaction (9) is suppressed after the abstraction of the hydrogen by the chlorine radical. Since the partial pressure of O_2 in the chamber is high, reaction (15) is more likely to occur

$$FC(O)OOC(O)OCH_2 + O_2 \rightarrow FC(O)OOC(O)OCH_2OO \quad (15)$$

Many authors have proposed that the fate of these peroxy-radicals is to be converted into oxy-radicals by either forming O_2, according to reaction (16), or reaction with $FC(O)OOC(O)OCH_2$ radicals (reaction 17).[39-41]

$$2\ FC(O)OOC(O)OCH_2OO \rightarrow 2\ FC(O)OOC(O)OCH_2O + O_2 \quad (16)$$

$$FC(O)OOC(O)OCH_2 + FC(O)OOC(O)OCH_2OO \rightarrow 2\ FC(O)OOC(O)OCH_2O \quad (17)$$

After the disappearance of the reactant, three bands are observed between 1800 and 1900 cm^{-1}, as shown in figure 5. This bands may be indicative of the presence of a molecule containing three C=O groups. In addition, a band at ~1178 cm^{-1} was observed, indicating the presence of a C—H bond, so the mechanism may continue through reaction (18):

$$FC(O)OOC(O)OCH_2O + Cl \rightarrow FC(O)OOC(O)OC(O)H + HCl \quad (18)$$

Another possible path for oxidation is the direct removal of OH from the peroxy-radical $FC(O)OOC(O)OCH_2OO$ as indicated in reaction (19).

$$FC(O)OOC(O)OCH_2OO \rightarrow FC(O)OOC(O)OC(O)H + OH \quad (19)$$

Reaction (18) has been proposed for other related species[42,43] and reaction (19) is also supported by other authors who proposed the hydrogen shifting from the carbon atom to the terminal oxygen. In our case, the radical HOOCHOC(O)OOC(O)F would be produced which will ultimately end up producing H(O)COC(O)OOC(O)F and OH.[44]

We performed frequency calculations for the H(O)COC(O)OOC(O)F molecule, finding three characteristic bands at 1953 (29), 1898 (16) and 1863 (40) cm^{-1} corresponding to the three

carbonyl groups in the molecule (relative intensities in parenthesis). In addition, two bands at 1177 (100) and a smaller one at 1234 (14) cm^{-1} were obtained and correspond to the O-C-O and O-C-F bendings.

This molecule could be susceptible of being attacked by Cl atoms and will most likely react to produce three molecules of CO_2 and a fluorine atom, as indicated in reactions (20) and (21).

$$H(O)COC(O)OOC(O)F + Cl \rightarrow C(O)OC(O)OOC(O)F + HCl \quad (20)$$

$$C(O)OC(O)OOC(O)F \rightarrow 3\ CO_2 + F \quad (21)$$

Fluorine may abstract hydrogen from the reagent, $FC(O)OOC(O)OCH_3$, forming HF as can be seen in figure 5. The great increase in the concentration of CO_2 showed in the figure is another evidence for the proposed mechanism in the presence of oxygen.

4. Conclusions

The reaction of the peroxide $FC(O)OOC(O)OCH_3$ with Cl atoms generated by the laser photolysis of Cl_2, in the absence of oxygen, results in the intermediates $FC(O)OOC(O)OCH_2Cl$, $FC(O)OOC(O)OCHCl_2$ and the product $FC(O)OOC(O)OCCl_3$; three novel compounds detected for the first time, using FTIR spectroscopy in conjunction with first principle calculations. The reaction proceeds by sequential chlorine substitution of hydrogen atoms with rate constants (4.0; 3.2 and 1.7) $\times 10^{-14}$ cm^3 $molecule^{-1}$ s^{-1} for the first, second and third abstraction respectively. A kinetic model was employed to simulate the evolution of the system confirming this sequence of reactions. From a statistical point of view the probability ratio for replacement in a —CH_3

fragment of the first and second hydrogen atoms is 3:2 = 1.5 and for the third is 3:1 = 3. The ratios of rate constants for these replacements in the title molecule are (4.0 : 3.2 = 1.25) and (4.0 : 1.7 = 2.35) indicating that the replacement reactions are somewhat different from the statistical probability. When the reaction is run in presence of oxygen the replacement reactions of Cl are suppressed and oxidation to (mainly) CO_2 and HCl takes place through highly oxidized intermediates with enough lifetime to be detected by FTIR spectroscopy.

Figure 1. Rate constants of the reaction Cl + $FC(O)OOC(O)OCH_3$ relative to $CHCl_3$ (green), CH_2Cl_2 (blue) y CH_4 (red) with a total pressure of 700 torr using N_2 as bath gas.

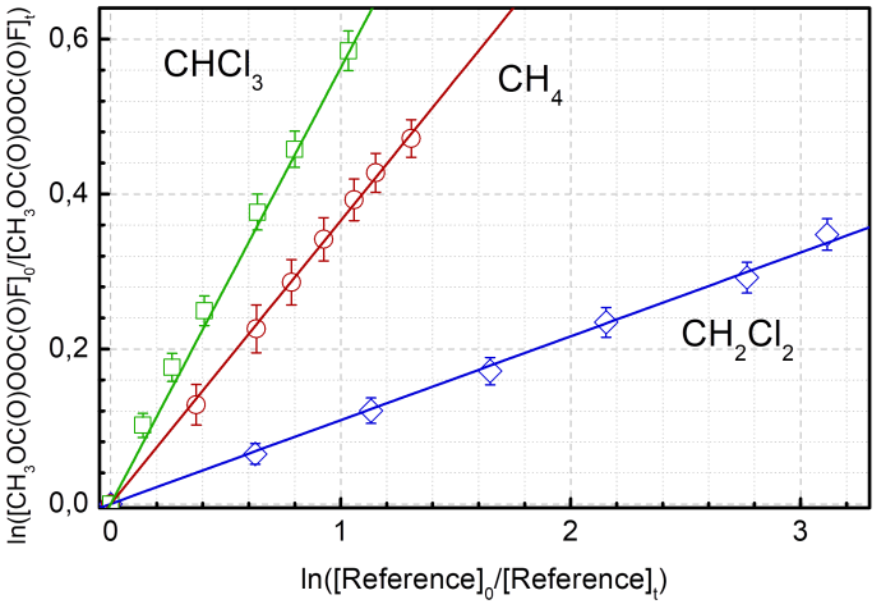

Figure 2. IR Spectrum progression of the reaction between $FC(O)OOC(O)OCH_3$ and Cl. $t_{a)}$ (0 μs) < $t_{b)}$ (4.5 μs) < $t_{c)}$ (7.5 μs).

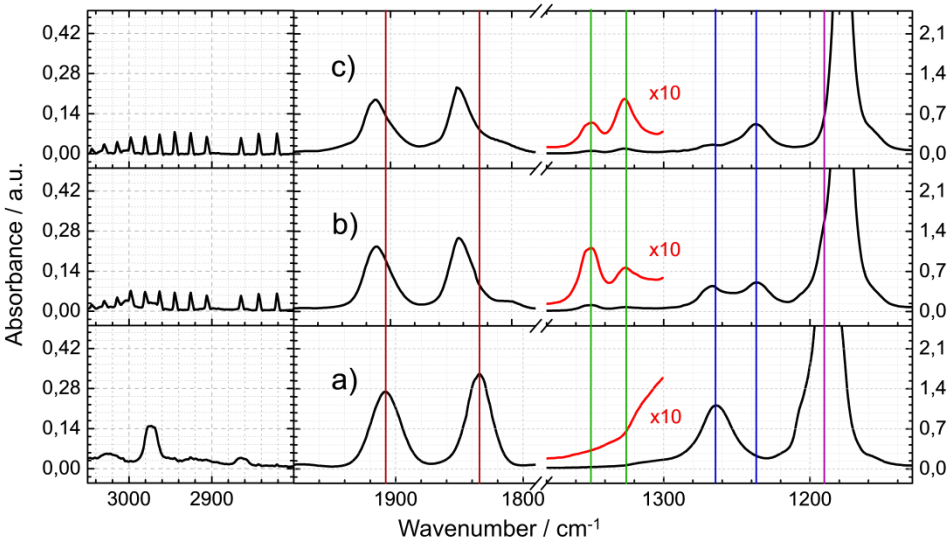

Figure 3. Plot of $(FC(O)OOC(O)OCH_2Cl)_t/(FC(O)OOC(O)OCH_3)_0$ vs. $\Delta(FC(O)OOC(O)OCH_3)/(FC(O)OOC(O)OCH_3)_0$ under different pressures of Cl_2 (○ 5 mbar, △ 30 mbar, ◇ 60 mbar, y ☆ 100 mbar, □ 130 mbar), following the bands 2973 cm^{-1} for the precursor/reference and 1350 cm^{-1} for the $FC(O)OOC(O)OCH_2Cl$.

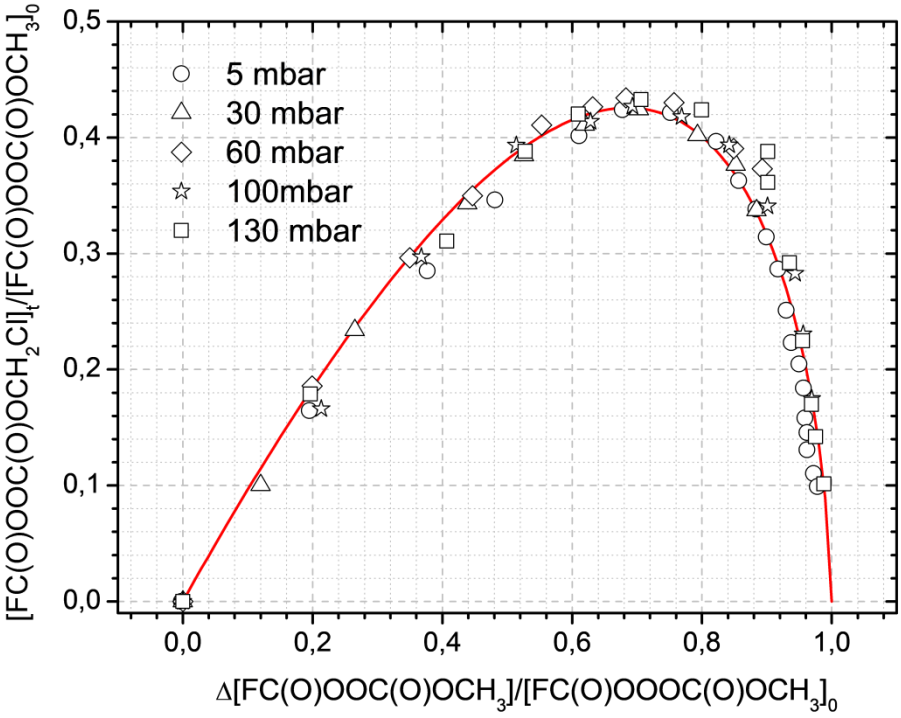

Figure 4. Concentrations vs reaction progression. Filled lines represent the simulation results at 25 °C using N_2 as gas bath. To calculate the concentrations of the different species the following bands were used: □ 2973, ◆ 2821, ▲ 1350, ▼ 1325, ● 2358 and ○ 842 cm^{-1}.

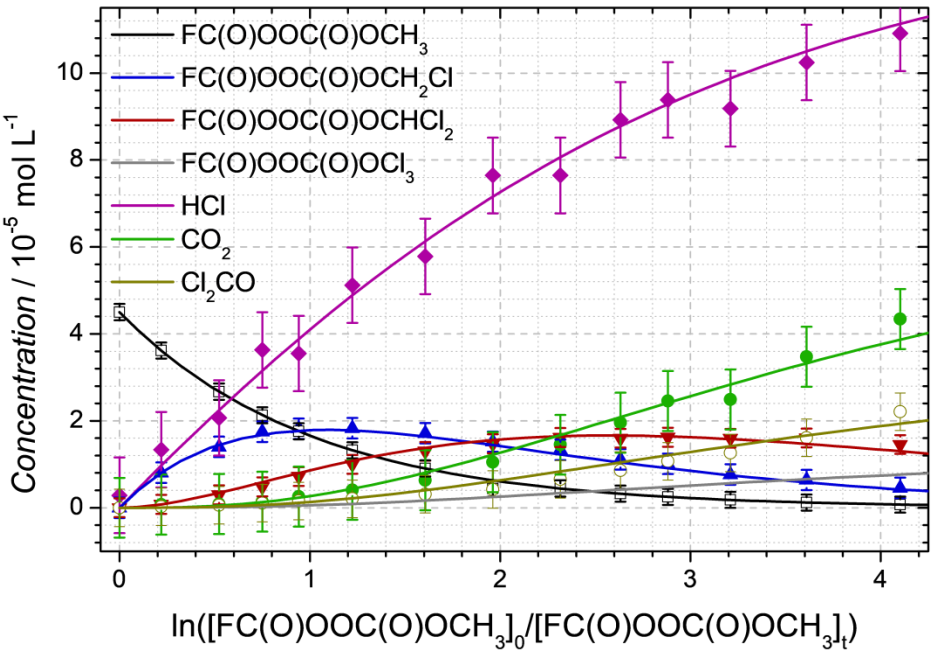

Figure 5. Initial (a) and final (b) IR Spectra of the reaction between $FC(O)OOC(O)OCH_3$ and Cl in the presence of O_2.

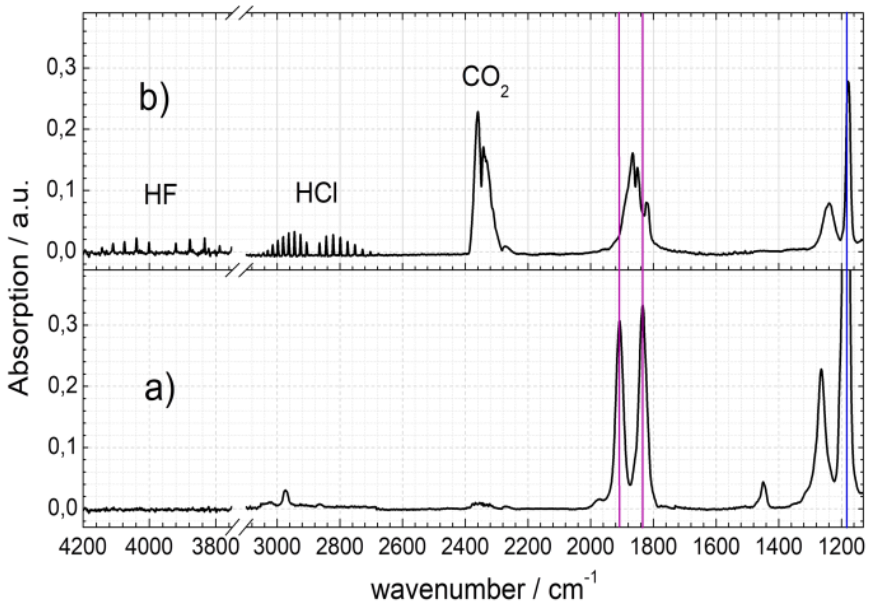

Table 1. Reaction mechanism and rate constants used in the simulation.

Reactions	Rate constant / cm^3 $molecule^{-1}$ s^{-1}	Ref.
$FC(O)OOC(O)OCH_3$ + Cl → $FC(O)OOC(O)OCH_2$ + HCl	4.0×10^{-14}	This work
$FC(O)OOC(O)OCH_2$ + Cl_2 → **$FC(O)OOC(O)OCH_2Cl$** + Cl	1.55×10^{-12}	[35]
$FC(O)OOC(O)OCH_2Cl$ + Cl → FC(O)OOC(O)OCHCl + HCl	3.2×10^{-14}	This work
FC(O)OOC(O)OCHCl + Cl_2 → **$FC(O)OOC(O)OCHCl_2$** + Cl	2.54×10^{-13}	[36]
$FC(O)OOC(O)OCHCl_2$ + Cl → $FC(O)OOC(O)OCCl_2$ + HCl	1.7×10^{-14}	From simulation
$FC(O)OOC(O)OCCl_2$ + Cl_2 → **$FC(O)OOC(O)OCCl_3$** + Cl	1.95×10^{-14}	[37]
$FC(O)OOC(O)OCCl_2$ → Cl_2CO + 2 CO_2 + F	1.5×10^{5} [a]	From simulation
$FC(O)OOC(O)OCH_3$ → H_2CO + 2 CO_2 + HF	1.8×10^{-5} [a]	[12]

[a]Rate constant for the unimolecular decomposition (s^{-1})

AUTHOR INFORMATION

Corresponding Author

* Corresponding Author: mburgos@fcq.unc.edu.ar

Author Contributions

The manuscript was written through contributions of all authors. All authors have given approval to the final version of the manuscript.

Funding Sources

Consejo Nacional de Investigaciones Científicas y Técnicas (CONICET), FONCyT, and SECyT-UNC.

Notes

There are no conflicts of interest to declare.

Supporting Information. (Figure S1) Simulation of radical-radical reactions. (Figure S2) Rate constant for the reaction 10 relative to reaction Cl + Reference. (Table S1) Calculated geometrical parameters of the most stable conformers. (Table S2) Calculated and experimental frequencies of the different peroxides.

ACKNOWLEDGMENT

Financial support from Consejo Nacional de Investigaciones Científicas y Técnicas (CONICET), FONCyT, and SECyT-UNC is gratefully acknowledged. M.B. is indebted to the CONICET for funding his Ph.D studies. Language assistance by translator M. F. Palmero is gratefully acknowledged.

REFERENCES

(1) Calvert, J.; Mellouki, A.; Orlando, J.; Pilling, M.; Wallington, T. *Mechanisms of Atmospheric Oxidation of the Oxygenates.* Oxford University Press: New York, **2011**.

(2) Argüello, G. A.; Willner, H. IR and UV Absorption Spectrum of the Trifluoromethoxy Radical, $CF_3O\cdot$, Isolated in Rare Gas Matrices. *J. Phys. Chem. A*, **2001**, *105*, 3466-3470.

(3) von Ahsen, S.; Willner, H.; Francisco, J. S. The Trifluoromethoxy Carbonyl Peroxy Radical $CF_3OC(O)OO$. *Chem. Eur. J.,* **2002**, *8*, 4675-4680.

(4) von Ahsen, S.; Hufen, J.; Willner, H.; Francisco, J. S. The Trifluoromethoxycarbonyl Radical CF_3OCO. *Chem. Eur. J.*, **2002**, *8*, 1189-1195.

(5) Hohorst, F. A.; DesMarteau, D. D.; Anderson, L. R.; Gould, D. E.; Fox, W. B. Reactions of Bis(trifluoromethyl) Trioxide. *J. Am. Chem. Soc.*, **1973**, *95*, 3866-3869.

(6) Arvía, A. J.; Aymonino, P. J.; Schumacher, H. J. Preparación y Propiedades del Peróxido de Bis(monofluorcarbonilo). *An. Asoc. Quim. Argent. (1921-2001),* **1962**, *50 (135-143)*, 1195-1203.

(7) Argüello, G. A.; Willner, H.; Malanca, F. E. Reaction of CF_3 Radicals with CO and O_2. Isolation of Bis(trifluoromethyl)peroxydicarbonate, $CF_3OC(O)OOC(O)OCF_3$, and Identification of Bis(trifluoromethyl)trioxydicarbonate, $CF_3OC(O)OOOC(O)OCF_3$. *Inorg. Chem.*, **2000**, *39*, 1195-1199.

(8) Argüello, G. A.; von Ahsen, S.; Willner, H.; Burgos Paci, M. A.; García, P. The Open-Chain Trioxide $CF_3OC(O)OOOC(O)OCF_3$. *Chem. Eur. J.*, **2003**, *9*, 5135-5141.

(9) Burgos Paci, M. A.; García, P.; Malanca, F. E.; Argüello, G. A.; Willner, H. Synthesis and Characterization of Trifluoromethyl Fluoroformyl Peroxycarbonate, $CF_3OC(O)OOC(O)F$. *Inorg. Chem*. **2003**, *42*, 2131-2135.

(10) Pernice, H.; Berkey, M.; Henkel, G.; Willner, H.; Argüello, G. A.; McKee, M. L.; Webb, T. R. Bis(fluorformyl)trioxid, FC(O)OOOC(O)F. *Angew. Chem.* **2004**, *116*, 2903-2906.

(11) Berasategui, M.; Burgos Paci, M. A.; Argüello, G. A. Isolation and Characterization of $CH_3OC(O)OOC(O)F$ from the Reaction CH_3OH + FC(O)OOC(O)F. *Z. Anorg. Allg. Chem*. **2012**, *638*, 547-552.

(12) Berasategui, M.; Burgos Paci, M. A.; Argüello, G. A. Properties and Thermal Decomposition of the Hydro-Fluoro-Peroxide $CH_3OC(O)OOC(O)F$. *J. Phys. Chem. A*, **2014**, *118*, 2167-2175.

(13) Finlayson-Pitts, B. J.; Pitts Jr, J. N. *Chemistry of the Upper and Lower Atmosphere*. Academic Press: San Diego, **2000**.

(14) Vijayakumar, S.; Rajakumar, B. Experimental and Theoretical Investigations on the Reaction of 1,3-Butadiene with Cl Atom in the Gas Phase. *J. Phys. Chem. A*, **2017**, *121*, 1976-1984.

(15) Poutsma, M. L. Evolution of Structure−Reactivity Correlations for the Hydrogen Abstraction Reaction by Chlorine Atom. *J. Phys. Chem. A*, **2013**, *117*, 687-703.

(16) Saiz-Lopez, A.; von Glasow, R. Reactive Halogen Chemistry in the Troposphere. *Chem. Soc. Rev*. **2012**, *41*, 6448-6472.

(17) Hong-Bin, X.; Fangfang, M.; Qi, Y.; Ning, H.; Jingwen, C. Computational Study of the Reactions of Chlorine Radicals with Atmospheric Organic Compounds Featuring NHx−π-Bond (x = 1, 2) Structures. *J. Phys. Chem. A*, **2017**, *121*, 1657-1665.

(18) Walavalkar, M. P.; Vijayakumar, S.; Sharma, A.; Rajakumar, B.; Dhanya, S. Is H Atom Abstraction Important in the Reaction of Cl with 1-Alkenes? *J. Phys. Chem. A*, **2016**, *120*, 4096-4107.

(19) Ezell, M. J.; Wang, W. H.; Ezell, A. A.; Soskin, G.; Finlayson-Pitts, B. Kinetics of Reactions of Chlorine Atoms with a Series of Alkenes at 1 atm and 298 K: Structure and Reactivity. *J. Phys. Chem. Chem. Phys.* **2002**, *4*, 5813-5820.

(20) Galán, E.; González, I.; Fabbri, B. Estimation of Fluorine and Chlorine Emissions from Spanish Structural Ceramic Industries. The Case Study of the Bailén Area, Southern Spain. *Atmos. Environ*. **2002**, *36*, 5289-5298.

(21) Thornton, J. A.; Kercher, J. P.; Riedel, T. P.; Wagner, N. L.; Cozic, J.; Holloway, J. S.; Dube, W. P.; Wolfe, G. M.; Quinn, P. K.; Middlebrook, A. M. Large Atomic Chlorine Source Inferred from Mid-Continental Reactive Nitrogen Chemistry. *Nature,* **2010**, *464*, 271-274.

(22) Young, C. J.; Washenfelder, R. A.; Edwards, P. M.; Parrish, D. D.; Gilman, B.; Kuster, W. C.; Mielke, L. H.; Osthoff, H. D.; Tsai, C.; Pikelnaya, O., et al. Chlorine as a Primary Radical: Evaluation of Methods to Understand its Role in Initiation of Oxidative Cycles. *Atmos. Chem. Phys*. **2014**, *14*, 3427-3440.

(23) Curtiss, L. A.; Raghavachari, K.; Trucks, G. W.; Pople, J. A. Gaussian-2 Theory for Molecular Energies of First- and Second-Row Compounds. *J. Chem. Phys*. **1991**, *94*, 7221-7230.

(24) Frisch, M. J.; Trucks, G. W.; Schlegel, H. B.; Scuseria, G. E.; Robb, M. A.; Cheeseman, J. R.; Scalmani, G.; Barone, V.; Mennucci, B.; Petersson, G. A., et al. *Gaussian 09, Revision A.02*; Gaussian, Inc.: Wallingford, CT, **2009**.

(25) Atkinson, R. Kinetics and Mechanisms of the Gas-Phase Reactions of the Hydroxyl Radical with Organic Compounds. *J. Phys. Chem.* Ref. Data, **1989**, Monograph 1.

(26) Atkinson, R.; Baulch, D. L.; Cox, R. A.; Hampson, R. F.; Kerr, J. A.; Rossi, M. J.; Troe, J. Evaluated kinetic, Photochemical and Heterogeneous Data for Atmospheric Chemistry: Supplement V - IUPAC Subcommittee on Gas Kinetic Data Evaluation for Atmospheric Chemistry. *J. Phys. Chem*. Ref. Data, **1997**, *26*, 521-1011.

(27) Burgos Paci, M.A.; Argüello, G. A. Kinetics of the Reaction Between CF_2O and CH_3OH. *Proc. Env. Simul. Chambers*. **2006**, 207-212.

(28) Mack, H.-G.; Della Vedova, C. O.; Oberhammer, H. Bis(fluorocarbony1) Peroxide; an Unusual Molecular Structure. *Angew. Chem. Int. Ed. Engl*. **1991**, *30*, 1145-1146.

(29) Kopitzky, R.; Willner, H.; Hermann, A.; Oberhammer, H. Bis(trifluoroacetyl) Peroxide, $CF_3C(O)OOC(O)CF_3$. *Inorg. Chem*. **2001**, *40*, 2693-2698.

(30) Hnyk, D.; Machacek, J.; Argüello, G. A.; Willner, H.; Oberhammer, H. Stucture and Conformational Properties of Bis(trifluoromethyl) Peroxydicarbonate, $CF_3OC(O)O$-$OC(O)OCF_3$. *J. Phys. Chem. A*, **2003**, *107*, 847-851.

(31) Oberhammer, H. Gas Phase Structures of Peroxides: Experiments and Computational Problems. *Chem. Phys. Chem*, **2015**, *16*, 282-290.

(32) Meagher, R. J.; McIntosh, M. E.; Hurley, M. D.; Wallington, T. J. A Kinetic Study of the Reaction of Chlorine and Fluorine Atoms with HC(O)F at 295 ± 2 K. *Int. J. Chem. Kinet.* **1997**, *29*, 619-625.

(33) Ianni, J. C. *Kintecus*, *version 5.5*; **2015**.

(34) Manion, J. A.; Huie, R. E.; Levin, R. D.; Burgess Jr., D. R.; Orkin, V. L.; Tsang, W.; McGivern, W. S.; Hudgens, J. W.; Knyazev, V. D.; Atkinson, D. B. et al. NIST Chemical Kinetics Database, NIST Standard Reference Database 17, Version 7.0 (Web Version), Release 1.6.8, National Institute of Standards and Technology, Gaithersburg, MD, http://kinetics.nist.gov/ (retrieved December, 2015).

(35) Eskola, A. J.; Timonen, R. S.; Marshall, P.; Chesnokov, E. N.; Krasnoperov, L. N. Rate Constants and Hydrogen Isotope Substitution Effects in the CH_3 + HCl and CH_3 + Cl_2 Reactions. *J. Phys. Chem. A,* **2008**, *112*, 7391-7401.

(36) Seetula, J. A. Kinetics of the R+Cl_2, (R = CH_2Cl, CHBrCl, CCl_3 and CH_3CCl_2) Reactions. An ab initio Study of the Transition States. *J. Chem. Soc. Farad. Trans*. **1998**, *94*, 3561-3567.

(37) Brudnik, K.; Twarda, M.; Sarzynski, D.; Jodkowski, J. T. Theoretical Study of the Kinetics of Chlorine Atom Abstraction from Chloromethanes by Atomic Chlorine. *J. Mol. Model.* **2013**, *19*, 4181-4193.

(38) Wallington, T. J.; Hurley, M. D.; Maurer, T.; Barnes, I.; Becker, K. H.; Tyndall, G. S.; Orlando, J. J.; Pimentel, A. S.; Bilde, M. Atmospheric Oxidation Mechanism of Methyl Formate. *J. Phys. Chem. A.* **2001**, *105*, 5146-5154.

(39) Noell, A. C.; Alconcel, L. S.; Robichaud, D. J.; Okumura, M.; Sander, S. P. Near-Infrared Kinetic Spectroscopy of the HO_2 and C_2H5O_2 Self-Reactions and Cross Reactions. *J. Phys. Chem. A*, **2010**, *114*, 6983-6995.

(40) Atkinson, R.; Baulch, D. L.; Cox, R. A.; Crowley, J. N.; Hampson Jr., R. F.; Kerr, J. A.; Rossi, M. J.; Troe, J. Summary of Evaluated Kinetic and Photochemical Data for Atmospheric Chemistry. **2001**, 1-56.

(41) Keiffer, M.; Miscampbell, A. J.; Pilling, M. J. A Global Technique for Analyzing Multiple Decay Curves. Application to the $CH_3 + O_2$ System. *J. Chem. Soc. Faraday Trans. 2*. **1988**, *84*, 505-514.

(42) Villano, S. M.; Huynh, L. K.; Carstensen, H. H.; Dean, A. M. High-Pressure Rate Rules for Alkyl + O_2 Reactions. 1. The Dissociation, Concerted Elimination, and Isomerization Channels of the Alkyl Peroxy Radical. *J. Phys. Chem. A*. **2011**, *115*, 13425-13442.

(43) Sheng, C. Y.; Bozzelli, J. W.; Dean, A. M.; Chang, A. Y. Detailed Kinetics and Thermochemistry of $C_2H_5 + O_2$: Reaction Kinetics of the Chemically-Activated and Stabilized CH_3CH_2OO Adduct. *J. Phys. Chem. A*. **2002**, *106*, 7276-7293.

(44) Sharma, S.; Raman, S.; Green, W. H. Intramolecular Hydrogen Migration in Alkylperoxy and Hydroperoxyalkylperoxy Radicals: Accurate Treatment of Hindered Rotors. *J. Phys. Chem. A*. **2010**, *114*, 5689-5701.

Table of Content Image (TOC)